Direct Ab Initio Dynamics Study on a Gas Phase Microsolvated S_N2 Reaction of $F^-(H_2O)$ with CH_3Cl

Hiroto Tachikawa*

Division of Molecular Chemistry, Graduate School of Engineering, Hokkaido University, Sapporo 060-8628, Japan

Received: August 27, 1999; In Final Form: November 2, 1999

A microsolvated S_N2 reaction of $F^-(H_2O)$ with CH_3Cl has been investigated by means of direct ab initio dynamics calculations in order to elucidate a detailed reaction mechanism. A full dimensional ab initio potential energy surface including all degrees of freedom was used in the dynamics calculations. Total energies and gradients were calculated at each time step. The vibrational phase of CH_3Cl was generated classically so as to take a temperature of 10 K. The dynamics calculations showed that three reaction channels are concerned with the reaction at a fixed collision energy (E_{coll} = 4.42 kcal/mol). These are expressed by $F^- + CH_3Cl \rightarrow CH_3F + Cl^- + H_2O$ (channel I), $F^- + CH_3Cl \rightarrow CH_3F + Cl^-(H_2O)$ (channel II), and $F^- + CH_3Cl \rightarrow CH_3F(H_2O) + Cl^-$ (channel III). Channel I is three-body dissociation of each product. In channels II and III, Cl^- and CH_3F, respectively, are solvated by a water molecule. It was found that the main reaction pathway is channels I and III, while channel II is significantly minor at E_{coll} = 4.42 kcal/mol. In all channels, the halogen exchange occurs rapidly with very short lifetimes of early and late complexes (i.e., the reaction proceeds via direct mechanism), which is similar to the nonsolvated reaction $F^- + CH_3Cl$. The preference of the reaction channels was discussed on the basis of theoretical results.

1. Introduction

Bimolecular nucleophilic substitution (S_N2) reactions in the gas phase have been the focus of extensive theoretical and experimental works in recent years due to their central importance in organic chemistry.[1,2] From a theoretical point of view, both ab initio MO, classical and quantum chemical dynamics calculations[2,3] have been extensively carried out by several groups. The energetics and potential energy surfaces (PESs) for the S_N2 reaction, $X^- + CH_3Y \rightarrow XCH_3 + Y^-$ (X = F, Cl and Y = F, Cl, Br), were calculated by the ab initio MO method. The reaction rates for several systems were calculated on the basis of transition state theory using the ab initio data.[4] For the dynamics features, conclusive works on the reaction dynamics of the gas-phase S_N2 reactions have been done by Hase and co-workers.[3] They calculated classical trajectories on the analytical PES fitted to ab initio calculations and showed that the reaction proceeds via a direct mechanism in which there is no long-lived complex on the entrance or exit region. They also found that there are multiple mechanisms for these reactions. For low reactant translation energies the reaction may occur either via trapping in the X- - -CH_3Y early-reaction complex, followed by non-RRKM dynamics or by a direct mechanism which is facilitated C−Y stretch excitation. High reactant translation energy also promotes a direct mechanism.

Recently, we have carried out direct ab initio dynamics calculations on a S_N2 reaction expressed by

$$F^- + CH_3Cl \rightarrow FCH_3 + Cl^-$$

using full-dimensional ab initio PES without analytical fitting.[5,6] In this method, the fitting of potential energy surface to ab initio data does not need, whereas the ab initio calculation of PES is carried out at each time step during the reaction. We found that the lifetimes of the complexes are very short enough to proceed via a direct mechanism. Also, it was found that the total available energy is partitioned into the relative translational mode between the products (43%) and into the C−F stretching mode (57%) at zero collision energy. The other internal modes of CH_3F remain in the ground state. These features are in good agreement with the previous dynamics studies by Hase and co-workers.[3]

More recently, Hase and co-workers carried out direct ab initio dynamics calculations of a symmetric S_N2 reaction of Cl^- with CH_3Cl.[3k] The collision energy they examined was as higher as 100 kcal/mol. They found that the trajectories were reacted by a backside attack mechanism, while reaction by front side attack was not observed.

From an experimental point of view, VanOrden et al.[7] measured the energy distribution of the products in the gas-phase S_N2 reaction ($F^- + CH_3Cl$) using Fourier transform ion cyclotron resonance (FT-ICR) spectroscopy. They showed that the reaction proceeds with a large fraction of the exothermicity partitioned into the relative translational energy of the products. This result is in reasonably agreement with the previous theoretical results by Hase and co-workers[3] and also by Tachikawa and Igarashi.[5,6]

Thus, a lot of works on the gas-phase S_N2 reaction for nonsolvated S_N2 reaction system have been carried out from both theoretical and experimental points of view.[2−6] Nevertheless, fewer studies have been addressed the role of solvation in gas-phase S_N2 reactions.[8,9] In particular, there is little information on the dynamics of microsolvated S_N2 reaction. From an experimental point of view, O'Hair et al. investigated solvent effects on a S_N2 reaction of fluoride ion with methyl chloride and measured the product ions formed by the reaction $F^-(H_2O) + CH_3Cl$.[11] They detected two ions, Cl^- and $Cl^-(H_2O)$, as products in the reaction. This result has been interpreted to show

* Corresponding author. E-mail: hiroto@eng.hokudai.ac.jp. Fax: +81-11-706-6750.

10.1021/jp993066t CCC: $19.00
Published on Web 12/28/1999

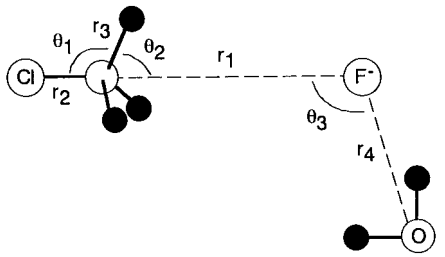

Figure 1. Geometrical parameters for the reaction system $F^-(H_2O) + CH_3Cl$.

that two reaction channels:

$$F^-(H_2O) + CH_3Cl \rightarrow CH_3F + Cl^- + H_2O \qquad \Delta H = -11 \text{ kcal/mol} \quad \text{(I)}$$

$$F^-(H_2O) + CH_3Cl \rightarrow CH_3F + Cl^-(H_2O) \qquad \Delta H = -24 \text{ kcal/mol} \quad \text{(II)}$$

are concerned with the microsolvated S_N2 reaction. Channel I is three-body dissociation reaction in which all species are separated from each other. In channel II, the product chloride ion is solvated by a water molecule. They estimated that the branching ratio of channels I/II is 3/1 (error bar is ±50%), although channel II is more favored in energy than channel I. This is an interesting point in this reaction. The energetics for the reaction $F^-(H_2O) + CH_3Cl$ were investigated by Hu and Truhlar using ab initio MO calculations.[12] The heats of reaction for channels I and II are calculated to be −2.0 and −17.4 kcal/mol at the MP2/aug-cc-pVTZ, respectively. However, the dynamic feature of the reaction (e.g., role of solvent molecule on the dynamics) is scarcely known because of a lack of direct trajectory study.

In the present study, direct ab initio dynamics calculation is applied to a microsolvated S_N2 reaction $F^-(H_2O) + CH_3Cl$ in order to elucidate the reaction mechanism. The purposes of this study are to elucidate the origin of the preference on the reaction channels and to elucidate the role of the solvent molecule in the reaction. In addition, the energy partitioning in the reaction is roughly estimated for the limited number of trajectories. Note that this work is the first attempt to calculate the trajectory for the microsolvated S_N2 reaction at the full ab initio MO level.

2. Methods

The classical trajectory calculations have been performed usually on an analytically fitted potential energy surface (PES) as previously carried out by several groups[14] and by us.[15] However, it is quite difficult to predetermine the reaction surfaces of the present systems due to the large number of degrees of freedom ($3N - 6 = 21$, where N is number of atoms in the system) and the asymmetric feature of PES. Therefore, in the present study, we applied the direct ab initio trajectory calculation on full dimensional PES with all degrees of freedom. The details of direct dynamics method and some examples are described elsewhere.[16]

In previous papers,[5,6] we showed that HF/3-21+G(d) calculation give a reasonable PES and dynamics features for the $F^- + CH_3Cl \rightarrow FCH_3 + Cl^-$ reaction. Also, this level of theory gave a good result for the $Cl^- + CH_3Cl$ reaction system.[3k] Therefore, we used 3-21+G(d) basis set in the direct ab initio dynamics calculations throughout. The HF/3-21+G(d) optimized geometry of CH_3Cl was chosen as an initial structure. The geometrical parameters for the reaction system are illustrated in Figure 1. The initial separation between $F^-(H_2O)$ and CH_3Cl and the position of H_2O relative to $F^-\cdots CH_3Cl$ were randomly generated in the range $r_1 = 6.20-8.20$ Å and $\theta_3 = 70-180°$. At the start of the trajectory calculation, atomic velocities of CH_3Cl were adjusted to give a temperature of 10 K as the classical vibrational distribution. The temperature of the system is defined by

$$T = \frac{1}{3Nk_B}\left\langle \sum_{i=1}^{N} m_i v_i^2 \right\rangle$$

where N is number of atoms, v_i and m_i are the velocity and mass of the ith atom, and k_B is Boltzmann's constant. The collision energy at the initial separation was fixed to 4.42 kcal/mol.

The equations of motion for n atoms in a molecule are given by

$$\frac{dQ_j}{dt} = \frac{\partial H}{\partial P_j}$$

$$\frac{\partial P_j}{\partial t} = -\frac{\partial H}{\partial Q_j} = -\frac{\partial U}{\partial Q_j}$$

where $j = 1 - 3N$, H is the classical Hamiltonian, Q_j is the cartesian coordinate of the jth mode, and P_j is the conjugated momentum. These equations were numerically solved by the Runge−Kutta method. No symmetry restriction was applied to the calculation of the gradients in the Runge−Kutta method. The time step size was chosen by 0.20 fs, and a total of 5000 steps were integrated for each dynamics calculation. The drift of the total energy is confirmed to be less than 1% throughout at all steps in the trajectory. To obtain the structures and energetics for the reaction system, ab initio MO calculations[17] were carried out for the stationary points along the reaction coordinate.

3. Results

A. Sample Trajectories. We have calculated 50 trajectories from the randomly selected initial configurations between CH_3F and $F^-(H_2O)$. Each molecule vibrates classically at 10 K before starting the reaction. The collision energy was fixed to $E_{coll} =$ 4.42 kcal/mol for all calculations. From the trajectory calculations, it was found that three reaction channels are concerned with the microsolvated S_N2 reaction $F^-(H_2O) + CH_3Cl$. These channels are expressed by

$$F^-(H_2O) + CH_3Cl \rightarrow CH_3F + Cl^- + H_2O \qquad \text{(channel I)}$$

$$\rightarrow CH_3F + Cl^-(H_2O) \qquad \text{(channel II)}$$

$$\rightarrow CH_3F(H_2O) + Cl^- \qquad \text{(channel III)}$$

Channel I is three-body dissociation in which the products ($CH_3F + Cl^- + H_2O$) leave from each other. In channel II, the Cl^- ion is solvated by the water molecule which forms $Cl^-\cdots H_2O$ complex as a product. The CH_3F molecule is solvated by a water molecule in channel III. The enthalpy for channel III is roughly estimated as −15.5 kcal/mol, and the solvation energy of $CH_3F\cdots H_2O$ is 5.5 kcal/mol at the MP2/aug-cc-pVDZ level. Those for channels I and II are experimentally obtained by −11 and −24 kcal/mol, respectively.

The dynamics calculations show that channel II is minor in the reaction, although it is energetically more favored than the other channels. The main reaction pathways are channels I and III which are direct dissociation and the complex formation of $CH_3F\cdots H_2O$, respectively. It was however impossible to distinguish experimentally these channels (I and III), because

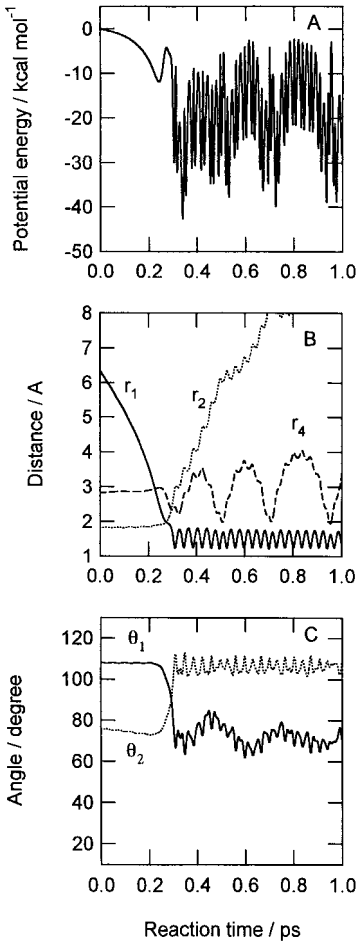

Figure 2. A typical trajectory for channel III. Potential energy of the system (A), interatomic distances (B), and angles (C) vs reaction time.

the Cl^- ion is only observed in the previous experiment.[11] In the following section, we show the profile of typical trajectories via channels I and III, and discuss the reaction mechanism in detail.

Sample Trajectory for Channel III. The profile of typical trajectory for channel III is given in Figure 2. Figure 2A shows the potential energy of the system (PE) calculated as a function of reaction time, while the nuclear distances and bond angles are plotted in parts B and C of Figure 2, respectively. The zero level of PE corresponds to the total energy at the initial separation ($F^-(H_2O) + CH_3Cl$). After starting the reaction, PE decreases gradually as a function of reaction time up to 0.23 ps. The time dependence of intermolecular distance (r_1) shows that $F^-(H_2O)$ gradually approaches CH_3F at this time region (0−0.23 ps). At 0.23 ps, the PE curve has the first energy minimum (−12 kcal/mol) which corresponds to the early complex expressed by $(H_2O)F^-\cdots CH_3F$. Actually, the intermolecular distances (r_1 and r_2) are calculated to be 2.864 and 1.8891 Å at 0.23 ps, respectively, which are close to the geometrical parameters for the early complex calculated by the static ab initio MO method.[6] Time period of the early complex region lies at 0.20−0.26 ps for this sample trajectory, suggesting that the lifetime of the early complex is very short (∼0.03 ps). At 0.30 ps, the trajectory reaches the higher energy point which corresponds to the saddle point (transition state, TS) of the reaction. In the vicinity of the TS state, the distances (r_1 and r_2) and the angles (θ_1 and θ_2) are largely changed by the halogen exchange and by the Walden inversion. Beyond the TS, PE drops suddenly to −43 kcal/mol, and then it vibrates strikingly at a high-frequency with a large amplitude. The trajectory enters the late complex region expressed by $(H_2O)FCH_3\cdots Cl^-$. At 0.35 ps, the intermolecular distances (r_1 and r_2) are calculated to be 1.485 and 2.688 Å, respectively, which are close to those of the late complex. The time dependence of bending angles (θ_1 and θ_2) at 0.2−0.4 ps indicates that the Walden inversion occurs with the halogen exchange between F^- and Cl^-. After the Walden inversion, the distance r_1 oscillates in the range 1.2244−1.7459 Å, suggesting that the C−F stretching mode of CH_3F is highly excited by the halogen exchange. For this trajectory, the C−F stretching mode of CH_3F is excited to $v = 7$. The time dependence of the distance r_2 indicates that Cl^- leaves monotonically from CH_3F as shown in Figure 2B. The relative velocity between Cl^- and $CH_3F(H_2O)$ is estimated by 950 m/s. The CH_3 umbrella mode of CH_3F vibrates in the range 101.6−111.6°, which corresponds to the vibrational ground state ($v = 0$). The C−H stretching mode of CH_3X (X = F and Cl) is still in the ground state before and after the reaction.

Next, we focus our attention on the position of H_2O during the reaction. The position of H_2O relative to F^- is defined by the distance r_4. The calculation shows that the distance r_4 is almost constant up to TS ($r_4 = 2.8$ Å). After TS, r_4 vibrates largely in the range 1.945−4.051 Å, suggesting that H_2O is bound to the F atom of CH_3F by a hydrogen bond, while the intermolecular stretching mode is highly excited.

The C−F bond (r_1) formed newly by the reaction vibrates in the range 1.2184−1.8059 Å at nascent state (time = 0.30−0.45 ps). At longer reaction time (time = 0.70−1.00 ps, i.e., the final state of the reaction), the amplitude of the C−F stretching mode decreases to 1.232−1.732 Å. On the other hand, the intermolecular distance between F and OH_2 (r_4) fluctuates in the range 2.226−3.534 Å at the nascent state, whereas it is enhanced to 1.945−4.051 Å at the final state. These results suggest that the excess energy of the C−F stretching mode of CH_3F, formed at nascent state of the exchange reaction, is transferred efficiently to the intermolecular vibrational mode between CH_3F and H_2O during the reaction. The relative translational energy between Cl^- and $CH_3F(H_2O)$ at the final state is estimated by 2.2 kcal/mol which is 5% of the total available energy.

Snapshots of the geometrical configurations for channel III are illustrated in Figure 3. At time zero, $F^-(H_2O)$ is located at $r_1 = 6.35$ Å. The F^- ion is solvated by the water molecule with a hydrogen bond, where one of the protons points toward F^-. The angle $CH_3F\cdots F\cdots H_2O$ ($=\theta_3$) is 148.1°. After starting the reaction, $F^-(H_2O)$ approaches gradually CH_3Cl and the trajectory enters the region of the early complex $(H_2O)F^-\cdots CH_3Cl$. An illustration at time 0.24 ps is one of the snapshots for the early complex. The structure at 0.28 ps is close to that of the TS in which the bending angle Cl−C−H is close to 90°. It should be noted that the skeleton of Cl−C−F is close to a collinear configuration in the vicinity of TS. The Walden inversion occurs at a very short time range, 0.28−0.30 ps, suggesting that this inversion occurs as a very fast process. The solvation structure of H_2O is drastically changed by proceeding the reaction. The proton of H_2O orients toward F^- at time zero. The H_2O molecule is rotated after the halogen exchange, while the oxygen atom points toward the F atom. This means that the solvation structure in $CH_3F\cdots H_2O$ is changed from the proton orientation form to the oxygen orientation form. This is due to the fact that charge on F is significantly changed from minus (F^-) to neutral (F atom) before and after the Walden inversion. The structural change for the solvation is clearly seen in the time range 0.30−0.38 ps. At 0.5 ps, Cl^- leaves from the $CH_3F\cdots H_2O$ complex, and it is fully separated at 1.0 ps.

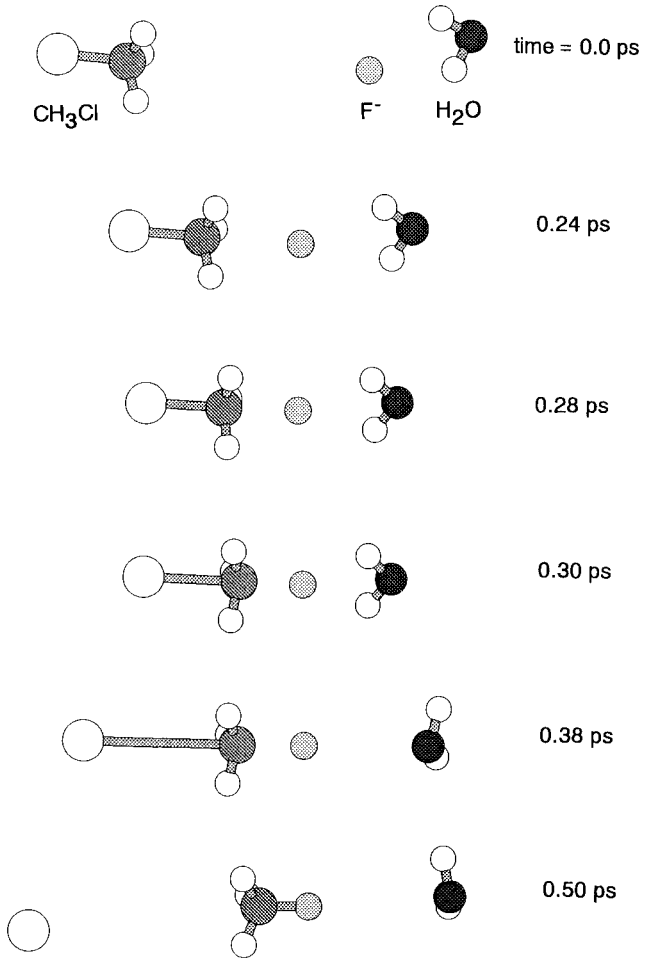

Figure 3. Snapshots of the conformations for the trajectory (channel III) illustrated as a function of reaction time.

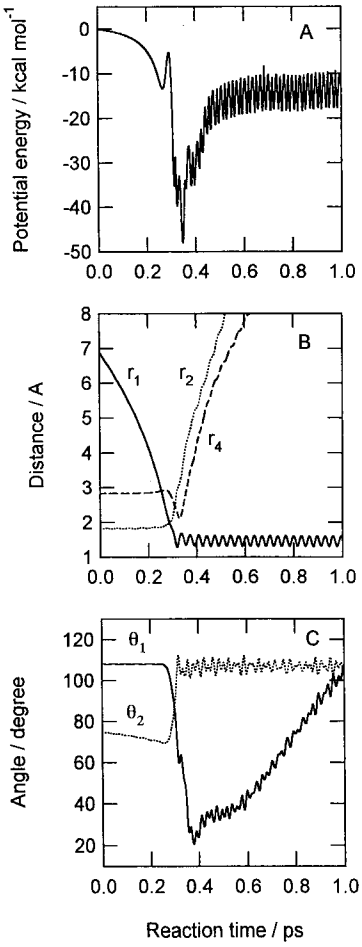

Figure 4. A typical trajectory for channel I. Potential energy of the system (A), interatomic distances (B), and angles (C) vs reaction time.

Sample Trajectory for Channel I. As described in the previous section, channel I (i.e., the direct three-body dissociation) plays an important role in the reaction as well as channel III. Hence, we show here the sample trajectory for channel I. The results are given in Figure 4. Figure 4A is the potential energy of the system (PE) calculated as a function of reaction time, while nuclear distances (r_1, r_2, and r_4) and bond angles (θ_1 and θ_2) are plotted in parts B and C of Figure 4, respectively. Zero level corresponds to the total energy of the reactant ($F^-(H_2O) + CH_3Cl$). PE decreases gradually to −12 kcal/mol where the trajectory enters the region of the early-complex. At 0.25 ps, the PE is minimized in this region. Immediately, the trajectory reaches to the transition state (TS). After that, it drops suddenly to −48 kcal/mol. This energy minimum corresponds to the late complex. The calculations show that the complex has a very short lifetime, and it is dissociated rapidly to three products ($Cl^- + H_2O + CH_3F$).

Time dependence of inter- and intramolecular distances are plotted as a function of time. At time zero, the intermolecular distance (r_1) is 6.82 Å, which is far enough to have no interaction between $F^-(H_2O)$ and CH_3Cl. After starting the reaction, the intermolecular distance $r_1 = r$(C−F) decreases gradually, meaning that $F^-(H_2O)$ approaches CH_3Cl. The distances r_2 and r_4 are almost constant up to TS. After TS, the distances r_2 and r_4 increase suddenly, meaning that the three-body dissociation, leading to the products ($Cl^- + H_2O + CH_3F$), occurs with the reaction. The relative velocity between CH_3F and Cl^- is estimated to be 2020 m/s which is about 2 times faster than that of channel III. The relative velocity between H_2O and $CH_3F(H_2O)$ is estimated by 1530 m/s. The C−F distance newly formed vibrates in the range 1.306−1.606 Å, meaning that the C−F stretching mode is vibrationally excited to $v = 2$. The CH_3 umbrella mode of CH_3F vibrates in the range 102.6−111.4°, which corresponds to the vibrational ground state ($v = 0$).

Snapshots of the geometrical configurations for channel I are illustrated in Figure 5. The F^- ion is solvated by H_2O at time zero, while the angle θ_3 is about 100° which is quite smaller than that of the sample trajectory for channel III. At 0.24 ps, F^- is close to CH_3Cl, but the angle θ_3 is still bent ($\theta_3 = 103.4°$) where one of the hydrogens of H_2O points toward F^-. At the transition state (time = 0.293 ps), the distances are calculated to be $r_1 = 1.8959$ Å and $r_2 = 2.0238$ Å. The F^- ion bonding to H_2O is located by r(F−O) = 2.7857 Å and the angle $\theta_3 = 27.5°$. After TS, both Cl^- and H_2O leave rapidly from CH_3F.

Summary of the Trajectory Calculations. A total of 50 trajectories were run from the initial configurations selected randomly. From the calculations, it was found that the most major reaction pathway is channels I and III in the reaction $F^-(H_2O) + CH_3Cl$. The relative populations of the internal states and the relative velocities between the products for channels I and III are given in Figure 6. Figure 6A shows the relative population of the C−F stretching mode of CH_3F. The quantum number is distributed from 2 to 10 with a peak of $v(C-F)_{str} = 5$. The average is $\langle v(C-F)_{str} \rangle = 5.5$. The quantum number for the CH_3 umbrella mode of CH_3F is distributed in the range $v = 0-7$ with a peak of $v = 2$, as shown in Figure 6B. The relative velocity between Cl^- and CH_3F is widely distributed

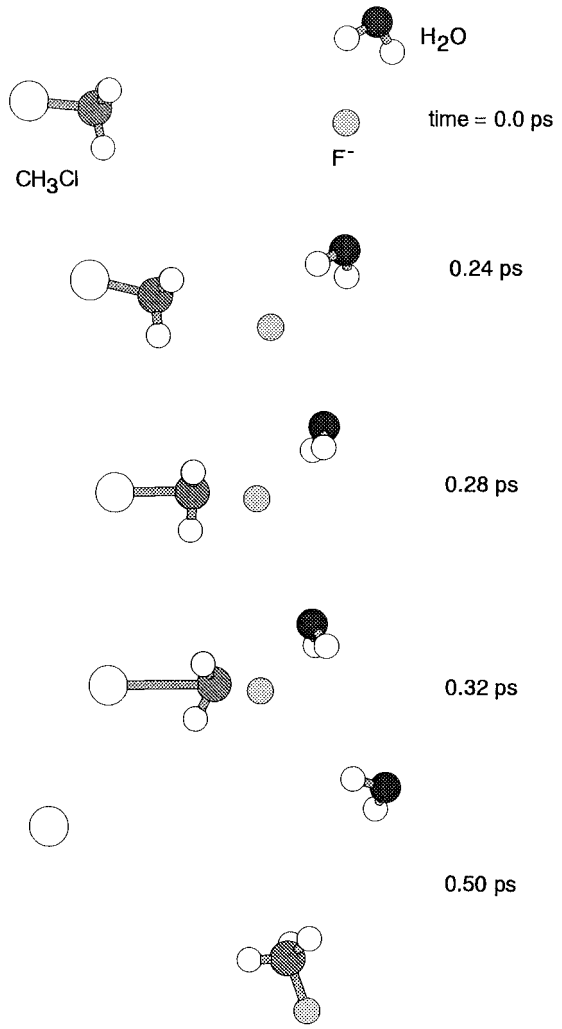

Figure 5. Snapshots of the conformations for the trajectory (channel I) illustrated as a function of reaction time.

from 600 to 2300 m/s with the average of velocity 1600 m/s, which corresponds to 6.53 kcal/mol as a relative translational energy. This means that 15% of the total available energy is partitioned into the relative translational energy and 85% of the energy is partitioned into the internal energy of CH_3F at the collision energy of 4.42 kcal/mol.

The populations of reaction channels, plotted as a function of angle F−C−O (=θ_3) at the initial separation, are given in Figure 7. The results were obtained at a fixed collision energy (E_{coll} = 4.42 kcal/mol). The population for channel III is widely distributed in the range θ_3 = 90−180°. On the other hand, the collisions of $F^-(H_2O)$ and CH_3Cl with both smaller angles (θ_3 = 90−110°) and near-collinear angles (θ_3 = 160−180°) lead to channel I. The angle leading to channel II is very narrow (θ_3 = 80−100°) as shown in Figure 7 (lower panel). The trajectory with the other angle, which is smaller than θ_3 = 80° leads to no reaction. The long-lived complex $ClCH_3F^-\cdots H_2O$ is formed in the case of θ_3 = 130−160°.

It should be noted that the present results are obtained at a fixed collision energy (E_{coll} = 4.42 kcal/mol) and a limited number of trajectories (50 trajectories). The branching ratio (I/III) and the angle dependency on the reaction channels are varied as a function of collision energy. A preliminary calculation of the same reaction system showed that the branching ratio (I/III) at higher collision energy (E_{coll} = 17.7 kcal/mol) is larger than that at the low collision energy.[18]

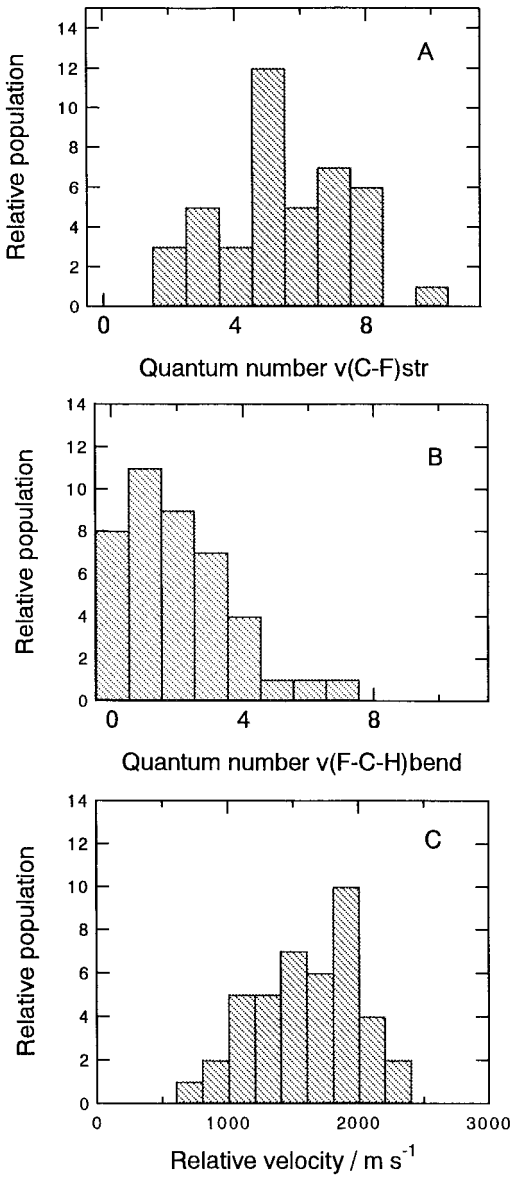

Figure 6. Relative populations of the vibrational and translational modes of the products formed by the microsolvated S_N2 reaction: (A) the C−F stretching mode of the product CH_3F; (B) CH_3 umbrella mode of the CH_3F; (C) relative velocity between Cl^- and $CH_3F(H_2O)$. The values are calculated direct ab initio dynamics calculations with a collision energy of 4.42 kcal/mol. The populations are calculated by 42 reactive trajectoies.

4. Discussion

Reaction Model. The present dynamics calculations showed that three reaction channels are competitive with each other in the S_N2 reaction $F^-(H_2O)$ + CH_3Cl. These channels are expressed by

$$F^-(H_2O) + CH_3Cl \rightarrow CH_3F + Cl^- + H_2O \quad \text{(channel I)}$$

$$\rightarrow CH_3F + Cl^-(H_2O) \quad \text{(channel II)}$$

$$\rightarrow CH_3F(H_2O) + Cl^- \quad \text{(channel III)}$$

The first channel is direct three-body dissociation of the products which proceeds directly without complex formation. In the second and third channels, the product Cl^- or CH_3F is solvated by H_2O. For all reaction channels, it was found that the halogen exchange proceeds via direct mechanism and that the early and

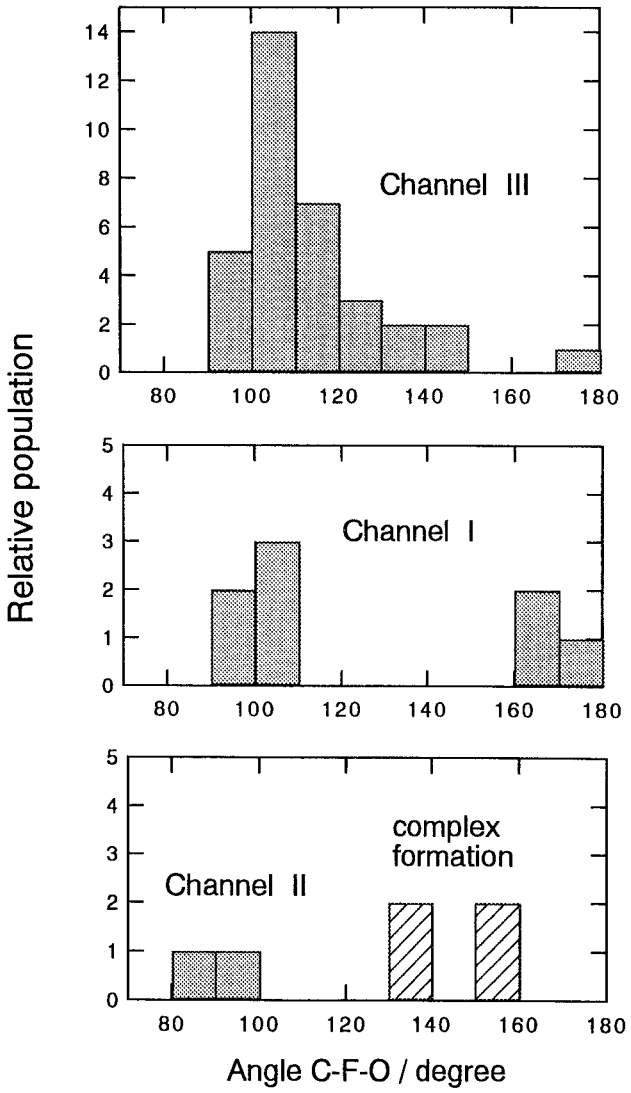

Figure 7. Population of trajectories leading to channels I, II, and III plotted as a function of angle C−F−O (=θ_3). The population of long-lived complex formation channel is also plotted. The values are calculated by 42 reactive trajectoies.

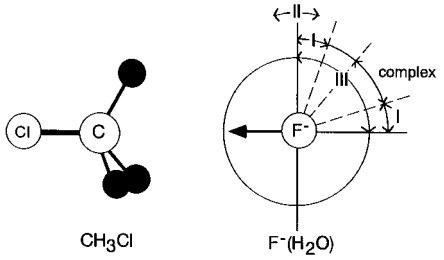

Figure 8. Reaction model for the microsolvated S_N2 reaction, $F^-(H_2O)$ + CH_3Cl. Circle means the position of H_2O around F^- at the initial separation.

late complexes have very short lifetimes. This feature is very similar to that of nonsolvated S_N2 reaction (F^- + $CH_3Cl \rightarrow CH_3F + Cl^-$).[3,5]

On the basis of the theoretical results, we propose a reaction model to explain the preference of the reaction channels. The dynamics calculations showed that the position of H_2O relative to the F···CH_3Cl molecular axis (i.e, angle θ_3) is mainly dominant in the reaction channels. Figure 8 shows the schematic illustration of the model derived from the present results. The circle around F^- means the position of H_2O relative to F^- at the initial separation between $F^-(H_2O)$ and CH_3Cl. The italic number and arrow indicate the product channel and angle region leading to its channel, respectively. The trajectories with larger angles (θ_3 = 160−180°) and smaller angles (θ_3 = 90−110°) lead mainly to the three-body dissociation channel (i.e, channel I). This is due to the fact that in the case of a collinear form (CH_3Cl···F^-···H_2O) the excess energy formed by the halogen exchange is directly and efficiently transferred to the CH_3F···H_2O intermolecular vibrational mode as well as the C−F stretching mode. Because of the vibrational excitation of intermolecular mode of CH_3F···H_2O, H_2O leaves easily from CH_3F without formation of $CH_3F(H_2O)$ complex. Also, channel I occurs with the collision angles in the range 90−110°. In such a collision, the H_2O molecule is scattered from CH_3F by the collision between $F^-(H_2O)$ and CH_3Cl. The H_2O molecule scattered is slightly rotated.

Channel III occurs at the wide angles in the range 90−180°. The H_2O molecule is still bound to F^- or F before and after collision, although the intermolecular mode of the complex CH_3F···H_2O is slightly excited because the excess energy is transferred to the intermolecular mode of the complex CH_3F···H_2O. Channel II (the product ion is $Cl^-(H_2O)$) occurs at the very narrow angles (θ_3 = 80−100°), meaning that the reaction probability for channel II is significantly small.

It should be noted that this model is limited to the reaction at low collision energy (around 5 kcal/mol). A preliminary calculation of the same reaction system showed that the branching ratio (I/III) is drastically varied as a function of collision energy; the ratio (I/III) becomes larger at higher collision energy.[18]

Comparison with the Experiments. The experiments for the microsolvated S_N2 reactions are limited. O'Hair et al. investigated the reaction $F^-(H_2O)$ + CH_3Cl using the tendem flowing afterglow selected ion flow tube technique.[11] They observed that the main product of the reaction is free Cl^- ion, whereas $Cl^-(H_2O)$ is minor. This result is in good agreement with the present calculations. Also, the present study predicts that the Cl^- ion is formed via channel II as well as channel I. To confirm the feature derived from the calculations, further experiment to ditect the product formed from channel III will be required.

The branching ratio of II/I has been estimated experimentally by 0.16−0.33 at 300 K.[11] This is inconsistent with our result (0.05) at a collision energy (E_{coll} = 4.42 kcal/mol). The deference may be mainly caused by the different collision energy. Trajectory calculations in the wide collision energies are now in progress.[18]

The effects of solvation, isotopic substitution, and temperature on the reaction of $F^-(H_2O)_n$ with CH_3Br (where n = 0−5) were investigated using a variable temperature-selected ion flow tube (SHIFT).[1u] The reaction rate for n = 0 (nonsolvent system) is about 3 times faster than that for n = 1, meaning that the additional water molecule decreases the reaction efficincy. The present calculations showed that eight trajectories lead to no reaction within 50 run of the trajectory calculations. These are mainly contributed from trajectories with smaller angles (80° < θ_3). To examine the effect of the water moelcule on the reaction provability, we calculated a trajectory using the same system but without water molecule. The trajectory leads to reactive collision, meaning that the water molecule prevents the reactive collision. Thus, the experimtent can be explained reasonably in terms of the model proposed in this work: the H_2O molecule prevents the reactive collision.

Comparison with the Previous Theoretical Works. The energetics and the structures at the transition state (TS) for the microsolvated S_N2 reactions, $X^-(H_2O)$ + CH_3Y, have been

calculated by Truhlar and co-workers.[12−14] For a microsolvated S_N2 reaction of $Cl^-(H_2O)$ with CH_3Cl, the symmetric TS structure with a C_{2v} symmetry was obtained by their ab initio MO calculations: the hydrogen atoms of H_2O are hydrogen bonded to each Cl^- at TS. However, for asymmetric S_N2 reaction $F^-(H_2O) + CH_3Cl$, the calculated saddle point geometry shows that the water molecule is still hydrogen bonded to the fluorine atom and does not interact with the Cl atom. They failed to find another saddle point that corresponds to the reaction with the water molecule moving in a concerted way from the fluorine atom side to the chloride atom side. Also, they pointed out a nonsynchronous reaction path in which the H_2O molecule is transferred to the Cl^- after the dynamical bottleneck to the reaction. Our dynamics calculations support strongly their prediction. Therefore, channel II is very minor in the reaction. Also, the present calculations indicate that the saddle point found by Thrular and co-workers corresponds to those of channels I and III, not for channel II. Channel II occurs after the dynamical bottleneck.

Concluding Remarks. We have introduced several approximations to calculate the potential energy surface and to treat the reaction dynamics. First, we assumed HF/3-21+G(d) multidimensional potential energy surface in the trajectory calculations throughout. As shown in previous papers,[5,6] the shape of PES for the $F^- + CH_3Cl$ reaction system calculated at the HF/3-21+G(d) level of theory is in good agreement with that of QCISD/6-311G(d,p) level. Therefore, it is enough to discuss qualitatively the reaction dynamics for the $F^-(H_2O) + CH_3Cl$ reaction system. However, more accurate wave function may provide deeper insight in the dynamics (for example, the branching ratio of the reaction channels).

Second, we calculated 50 trajectories at a fixed collision energy ($E_{coll} = 4.42$ kcal/mol). The number of trajectories may be enough to allow us to discuss the qualitative features of the dynamics, but many more are required to accurately compute the branching ratio for the reaction channels. This ratio would also vary greatly as a function of the collision energy. Despite several assumptions introduced here, the results enable us to obtain valuable information on the mechanism of the microsolvated S_N2 reaction.

Acknowledgment. The author is indebted to the Computer Center at the Institute for Molecular Science (IMS) for the use of the computing facilities. We also acknowledge partial support from a Grant-in-Aid from the Ministry of Education, Science, Sports and Culture of Japan. The author also acknowledges Mr. Manabu Igarashi for helping with data analysis.

References and Notes

(1) For a selection of recent experimental work on the gas-phase S_N2 reaction, see: (a) Olmstead, W. N.; Brauman, J. I. *J. Am. Chem. Soc.* **1997**, *99*, 4219. (b) Su, T.; Morris, R. A.; Viggiano, A. A.; Paulson, J. F. *J. Phys. Chem.* **1990**, *94*, 8426. (c) Viggiano, A. A.; Paschkewitz, J. S.; Morris, R. A.; Paulson, J. F.; Gonzalez-Lafont, A.; Truhlar, D. G. *J. Am. Chem. Soc.* **1991**, *113*, 9404. (d) DePuy, C. H.; Gronert, S.; Mullin, A.; Bierbaum, V. M. *J. Am. Chem. Soc.* **1990**, *112*, 8650. (e) Gronert, S.; DePuy, C. H.; Bierbaum, V. M. *J. Am. Chem. Soc.* **1991**, *113*, 4009. (f) Graul, S. T.; Bowers, M. T. *J. Am. Chem. Soc.* **1991**, *113*, 9696. (g) Graul, S. T.; Bowers, M. T. *J. Am. Chem. Soc.* **1994**, *116*, 3875. (h) Van Orden, S. L.; Pope, R. M.; Buckner, S. W. *Org. Mass Spectrom.* **1991**, *26*, 1003. (i) Cyr, D. M.; Posey, L. A.; Bishea, G. A.; Han, C.-C.; Johnson, M. A. *J. Am. Chem. Soc.* **1991**, *113*, 9697. (j) Cyr, D. M.; Bishea, G. A.; Scarton, M. G.; Johnson, M. A. *J. Chem. Phys.* **1992**, *97*, 5911. (k) Giles, K.; Grimsrud, E. P. *J. Phys. Chem.* **1992**, *96*, 6680. Knighton, W. B.; Boghar, J. A.; O'Connor, P. M.; Grimsrud, E. P. *J. Am. Chem. Soc.* **1993**, *115*, 12079. (l) Sahlstrom, K. E.; Knighton, W. B.; Grimsrud, E. P. *J. Phys. Chem. A* **1997**, *101*, 1501. (m) Viggiano, A. A.; Morris, R. A.; Paschkewitz, J. S.; Paulson, J. F. *J. Am. Chem. Soc.* **1992**, *114*, 10477. (n) Wladkowski, B. D.; Lim, K. F.; Allen, W. D.; Brauman, J. I. *J. Am. Chem. Soc.* **1992**, *114*, 9136. (o) Viggiano, A. A.; Morris, R. A.; Su, T.; Wladkowski, B. D.; Craig, S. L.; Zhong, M.; Brauman, J. I. *J. Am. Chem. Soc.* **1994**, *116*, 2213. (p) Craig, S. L.; Brauman, J. I. *Science* **1997**, *276*, 1536. (q) Viggiano, A. A.; Morris, R. A. *J. Phys. Chem.* **1994**, *98*, 3740. (r) Li, C.; Ross, P.; Szulejko, J. E.; McMahon, T. B. *J. Am. Chem. Soc.* **1996**, *118*, 9360. (s) Craig, S. L.; Brauman, J. I. *J. Phys. Chem. A* **1997**, *101*, 4745. (t) DeTuri, V. F.; Hintz, P. A.; Ervin, K. M. *J. Phys. Chem. A* **1997**, *101*, 5969. (u) Seeley, J. V.; Morris, R. A.; Viggiano, A. A.; Wang, H.; Hase, W. L. *J. Am. Chem. Soc.* **1997**, *119*, 577. (v) Le Garrec, J.-L.; Rowe, B. R.; Queffelec, J. L.; Mitchell, J. B. A.; Clary, D. C. *J. Chem. Phys.* **1997**, *107*, 1021. (w) Chabinyc, M. L.; Craig, S. L.; Regan, C. K.; Brauman, J. I. *Science* **1998**, *279*, 1882.

(2) For a selection of recent theoretical studies of S_N2 reactions, see: (a) Ryaboy, V. M. In *Advances in Classical Trajectory Methods*; Hase, W. L., Ed.; JAI Press: Greenwich, CT, 1994; Vol. 2, pp 115−145. (b) Vande Linde, S. R.; Hase, W. L. *J. Phys. Chem.* **1990**, *94*, 2778. (c) Tucker, S. C.; Truhlar, D. G. *J. Am. Chem. Soc.* **1990**, *112*, 3338. (d) Billing, G. D. *Chem. Phys.* **1992**, *159*, 109. (e) Wladkowski, B. D.; Allen, W. D.; Brauman, J. I. *J. Phys. Chem.* **1994**, *98*, 13532. (f) Wang, H.; Zhu, L.; Hase, W. L. *J. Phys. Chem.* **1994**, *98*, 1608. (g) Wang, H.; Hase, W. L. *J. Am. Chem. Soc.* **1995**, *117*, 9347. (h) Hu, W.-P.; Truhlar, D. G. *J. Am. Chem. Soc.* **1995**, *117*, 10726. (i) Glukhovtsev, M. N.; Pross, A.; Radom, L. *J. Am. Chem. Soc.* **1995**, *117*, 2024. (j) Glukhovtsev, M. N.; Pross, A.; Radom, L., *J. Am. Chem. Soc.* **1996**, *118*, 6273. (k) Wang, H.; Hase, W. L. *Chem. Phys.* **1996**, *212*, 247. (l) Clary, D. C.; Palma, J. J. *Chem. Phys.* **1996**, *106*, 575. (m) Wang, H.; Goldfield, E. M.; Hase, W. L. *J. Chem. Soc., Faraday Trans.* **1997**, *93*, 737. (n) Botschwina, P.; Horn, M.; Seeger, S.; Oswald, R. *Ber. Bunsen-Ges. Phys. Chem.* **1997**, *101*, 387. (o) Baer, T.; Hase, W. L. In *Unimolecular Reaction Dynamics-Theory and Experiments*; Oxford: New York, 1996.

(3) Trajectory studies for the S_N2 reaction: (a) Vande Linde, S. R.; Hase, W. L. *J. Phys. Chem.* **1990**, *94*, 6148. (b) Vande Linde, S. R.; Hase, W. L. *J. Chem. Phys.* **1990**, *93*, 7962. (c) Peslherbe, G. H.; Wang, H.; Hase, W. L. *J. Chem. Phys.* **1995**, *102*, 5626. (d) Cho, Y. J.; Vande Linde, S. R.; Zhu, L.; Hase, W. L. *J. Chem. Phys.* **1992**, *96*, 8275. (e) Hase, W. L.; Cho, Y. J. *J. Chem. Phys.* **1993**, *98*, 8626. (f) Wang, H.; Peslherbe, G. H.; Hase, W. L. *J. Am. Chem. Soc.* **1994**, *116*, 9644. (g) Peslherbe, G. H.; Wang, H.; Hase, W. L. *J. Am. Chem. Soc.* **1996**, *118*, 2257. (h) Hase, W. L. *Science* **1994**, *266*, 998. (i) Wang, H. Hase, W. L. *Int. J. Mass Spectrom. Ion Processes* **1997**, *167/168*, 573. (j) Mann, D. J. Hase, W. L. *J. Phys. Chem. A* **1998**, *102*, 6208. (k) Li, G.; Hase, W. L. *J. Am. Chem. Soc.* **1999**, *121*, 7124.

(4) (a) Wang, H.; Hase, W. L. *J. Am. Chem. Soc.* **1997**, *199*, 3093. (b) Craig, S. L.; Brauman, J. I. *J. Phys. Chem. A* **1997**, *101*, 4745.

(5) Tachikawa, H.; Igarashi, M. *Chem. Phys. Lett.* **1999**, *303*, 81.

(6) Igarashi, M.; Tachikawa, H. *Int. Mass Spectrom.* **1998**, *181*, 151.

(7) VanOrden, S. L.; Pope, R. M. Buckner, S. W. *Org. Mass Spectrom.* **1991**, *26*, 1003.

(8) van der Wel, H.; Nibbering, N. M. M.; Sheldon, J. C.; Hayes, R. N.; Bowie, J. H. *J. Am. Chem. Soc.* **1994**, *116*, 3609.

(9) (a) Gonzalez-Lafont, A.; Truong, T. N.; Truhlar, D. G. *J. Phys. Chem.* **1991**, *95*, 4618. (b) Zhao, X. G.; Lu, D.-H.; Liu, Y.-P.; Lynch, G. C.; Truhlar, D. G. *J. Chem. Phys.* **1992**, *97*, 6369.

(10) (a) Cossi, M.; Adamo, C.; Barone, V. *Chem. Phys. Lett.* **1998**, *297*, 1. (b) Kozaki, T.; Morihashi, K.; Kikuchi, O. *J. Am. Chem. Soc.* **1989**, *111*, 1547.

(11) O'Hair, R. A. J.; Davico, G. E.; Hacaloglu, J.; Dang, T. T.; DePuy, C. H.; Bierbaum, V. *J. Am. Chem. Soc.* **1994**, *116*, 3609.

(12) Hu, W.-P.; Truhlar, D. G. *J. Am. Chem. Soc.* **1994**, *116*, 7797.

(13) Zhao, X. G.; Tucker, S. C.; Truhlar, D. G. *J. Am. Chem. Soc.* **1991**, *113*, 826.

(14) Karplus, M.; Porter, R. N.; Sharm, R. D. *J. Chem. Phys.* **1965**, *43*, 3259.

(15) (a) Tachikawa, H. *J. Chem. Phys.* **1998**, *108*, 3966. (b) Tachikawa, H. *J. Phys. B* **1999**, *32*, 1451. (c) Tachikawa, H. *J. Phys. Chem.* **1995**, *99*, 225. (d) For a review article, see: H. Tachikawa, *Trends Phys. Chem.* **1997**, *6*, 279.

(16) (a) Tachikawa, H. *J. Phys. Chem. A* **1998**, *102*, 7065. (b) Tachikawa, H.; Igarashi, M. *J. Phys. Chem. A* **1998**, *102*, 8648. (c) Tachikawa, H. *J. Phys. Chem. A* **1997**, *101*, 7475. (d) Tachikawa, H. *J. Phys. Chem. A* **1999**, *103*, 6873. (e) Tachikawa, H. *Phys. Chem. Chem. Phys.* **1999**, *1*, 2675. (f) Tachikawa, H. *Phys. Chem. Chem. Phys.* **1999**, *1*, 4925. (g) Program code of the direct ab initio dynamics calculation was created by our group.

(17) Ab initio MO calculation program: Frisch, M. J.; Trucks, G. W.; Schlegel, H. B.; Gill, P. M. W.; Johnson, B. G.; Robb, M. A.; Cheeseman; J. R.; Keith, T.; Petersson, G. A.; Montgomery, J. A.; Raghavachari, K.; Al-Laham, M. A.; Zakrzewski, V. G.; Ortiz, J. V.; Foresman, J. B.; Cioslowski, J.; Stefanov, B. B.; Nanayakkara, A.; Challacombe, M.; Peng, C. Y.; Ayala, P. Y.; Chen, W.; Wong, M. W.; Andres, J. L.; Replogle, E. S.; Gomperts, R.; Martin, R. L.; Fox, D. J.; Binkley, J. S.; Defrees, D. J.; Baker, J.; Stewart, J. P.; Head-Gordon, M.; Gonzalez, C.; Pople, J. A.: *Gaussian 94*, revision D.3; Gaussian, Inc.: Pittsburgh, PA, 1995.

(18) Tachikawa, H. To be published.